MSM71/LOBSTER: Crust and upper mantle structure of the Ligurian Sea revealed by ambient noise tomography using ocean bottom seismometer data

Felix Noah Wolf[1,*], Dietrich Lange[1], Anke Dannowski[1], Martin Thorwart[2], Wayne Crawford[3], Lars Wiesenberg[2], Ingo Grevemeyer[1], Heidrun Kopp[1,2] and the AlpArray Working Group

[1]GEOMAR Helmholtz Centre for Ocean Research Kiel; [2]Kiel University;
[3]Laboratoire de Geosciences Marines, Institut de Physique du Globe de Paris, Paris.
*corresponding author: fnwolf@geomar.de

Introduction and Data

The opening history of the Liguro-Provencal backarc basin, which formed in conjunction with the Apennines-Calabrian subduction (Rollet et al., 2002 and Fig. 1), is key to understanding the transition from continental to oceanic domains in the Ligurian Sea.
We use ambient noise tomography, a method established for onshore data, but seldom used on ocean bottom seismometer (OBS) data, to image the crustal and upper mantle structure. Data from 22 OBS from the AlpArray offshore component LOBSTER and 22 temporary land stations from the AlpArray network (Fig. 2) in addition to 42 permanent land stations were available for the study.
This poster summarizes the paper of Wolf et al. (2021).

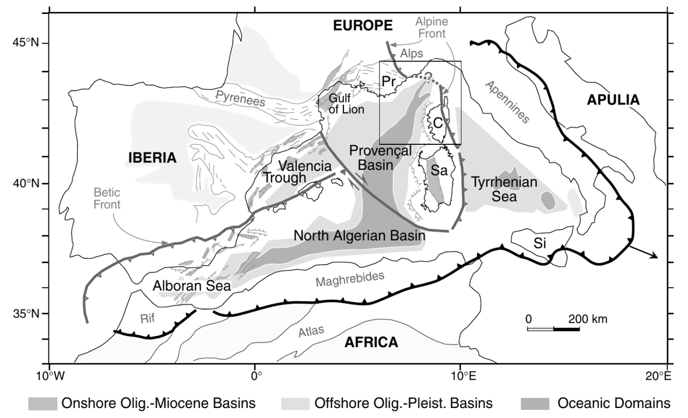

Fig. 1: (left) *Geological map of the region (Rollet, 2002).*

Fig. 2: (right) *Map of the study area and stations used. The OBS were deployed in June 2017 by the French RV Pourquois Pas? and recovered in February 2018 by the German RV Maria S. Merian.*

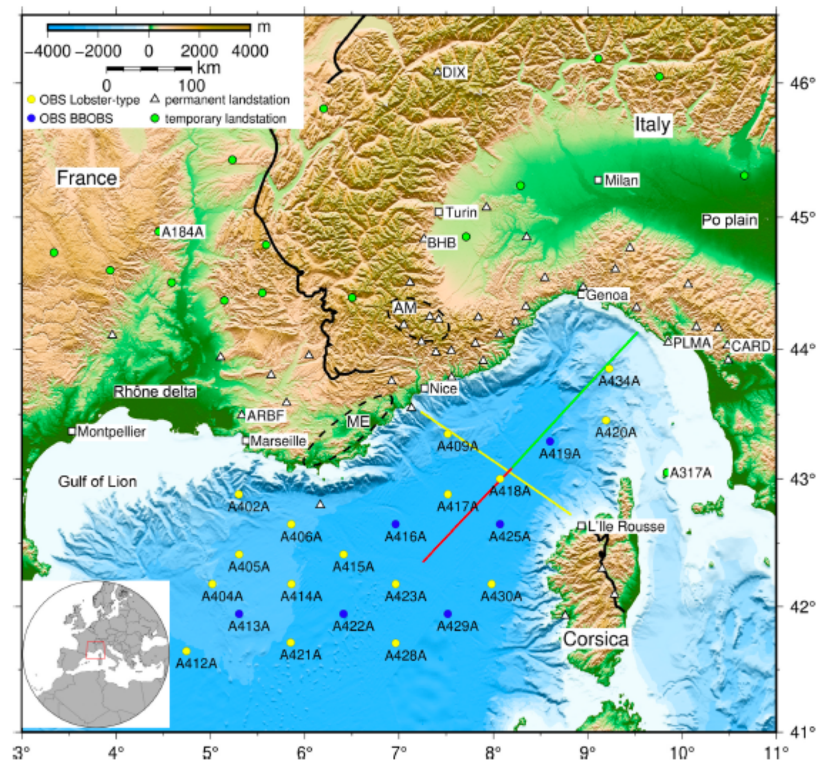

Methods

- Ambient Noise Tomography makes use of that part of seismological records, that - in earthquake studies - is called noise.
- By correlating the noise part of the signal one can estimate an empirical Green's function. Our processing follows Bensen et al. (2007). In addition to that, we remove compliance and tilt noise on the OBS after Crawford and Webb (1998, 2000).
- Compliance is a seafloor displacement caused by ocean surface waves, that introduce additional instrument acceleration (see Fig. 3 and 4).
- Cross-correlation functions of the corrected data were estimated for OBS-OBS and OBS-land station pairs (Fig. 5B). Additionally, land-OBS and land-land station pairs were calculated for A317A, ARBF and DIX.
- We derived Rayleigh wave group velocity dispersion curves using a multiple frequency technique (MFT) tool from Kiel University (based on Dziewonski, 1969). Examples are shown in Fig. 5B. We revised all dispersion curves manually, resulting in 1429 station pairs being used for the ambient noise tomography.
- For periods >20 s, we correlate 45 min recordings that include teleseismic events (1237 station pairs).

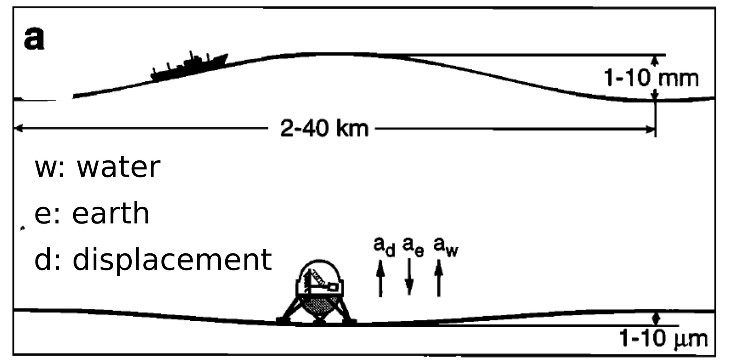

Fig. 3: (left) *Sketch of seafloor displacement caused by compliance (after Crawford et al., 1998).*

Fig. 4: *(right) Vertical component of OBS A404A on November 16th 2017 before (green) and after (black) compliance and tilt correction.*

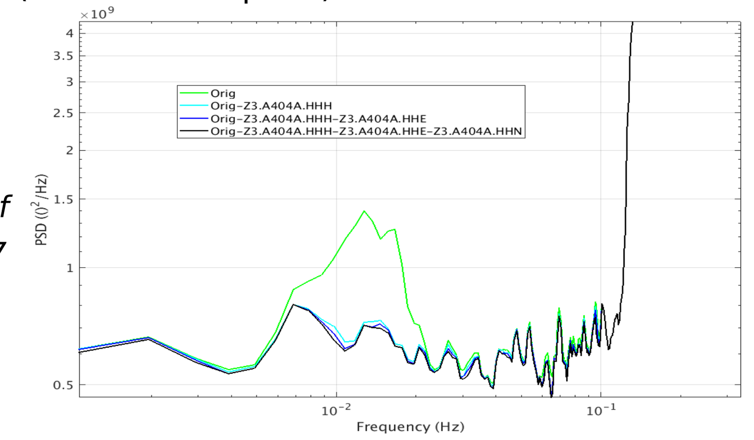

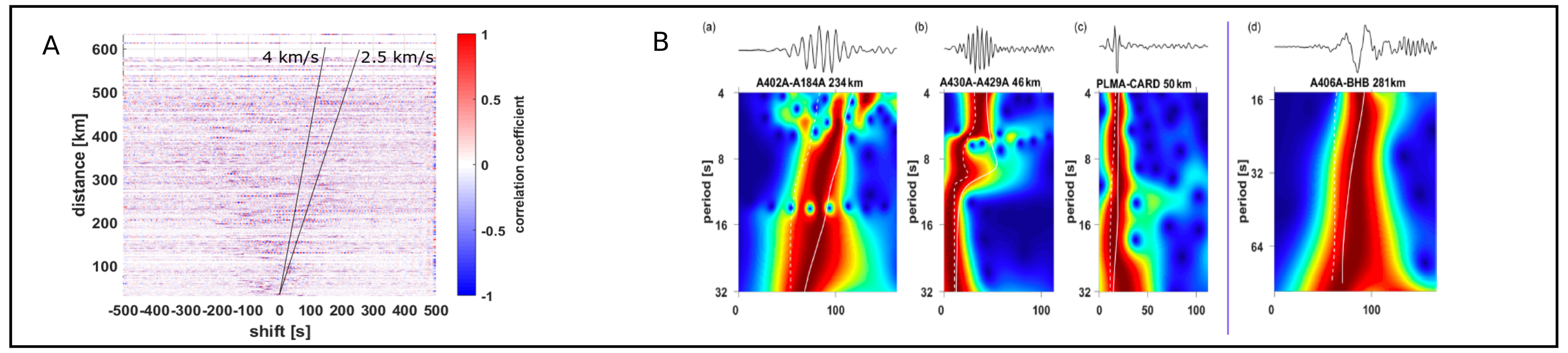

Fig. 5: *A) shows a section plot for all ambient noise station pairs. B) MFT examples for correlations on (a) OBS–land pair, (b) OBS–OBS pair, (c) land–land pair (all ambient noise cross-correlations), and (d) OBS–land station pair (cross-correlation containing teleseismic event). The solid white line shows the theoretical fundamental mode; the dashed white line shows the theoretical first higher mode. In (a), (c), and (d), the theoretical fundamental mode fits the theoretical velocities. In (b), the theoretical first higher mode correlates most strongly. Therefore, pair (b) was excluded from the tomography.*

Ambient Noise Tomography

- The dispersion curves are derived from cross-correlating ambient noise and teleseismic earthquakes (Fig. 7).
- Based on the dispersion curves picked from the MFT plots (Figs. 6 & 7), we inverted shear-wave velocities maps foreach period (Fig. 8).
- Fig. 8 shows group velocity (v_g) maps.
- For periods >= 20 s, the resolved area is small and homogenous. Starting at 40 s, we observe mantle velocities exceeding 4 km/s.

1D depth inversion

- We use the 2D group velocity maps as input for 1D depth inversion.
- We set up dispersion-files for every grid point of the map that include the group velocity and the standard deviation (used as uncertainty).
- The starting model is based on PREM and Dannowski et al. (2019).
- The 1D depth inversion (based on Herrmann, 2013) is calculated for every point seperately, taking into account the local topography.
- The water column is considered by using the water depth of the corresponding grid point.
- The resulting shear velocities (v_s) are shown as 2D maps (Fig. 9) and the chckerbord tests in Fig. 8.

Conclusions

The velocity model reveals a high-velocity area at the Argentera Massif, approximately 10 km below sea level. Offshore, the lithospheric structure in the Ligurian Basin mostly mimics the geometry of the basin. Shear-wave velocity maps indicate a gradual deepening of the Moho from 12–15 km in the south-western basin centre towards 20–25 km in the north-eastern basin and a more rapid deepening from the basin axis to the Provencial coast (>30 km). Based on the low v_p/v_s ratios of 1.74, we exclude mantle serpentinisation in the basin centre. Overall, the off-shore region north of Corsica is faster than the south-western basin at shallow depths (<12 km) and slower at greater depth. This is linked to the varying sediment cover and the crustal thickness. In the south-western part, the opening of the basin is more developed, but we do not observe oceanic crust.

This poster summarizes the findings published in Wolf et al. (2021).

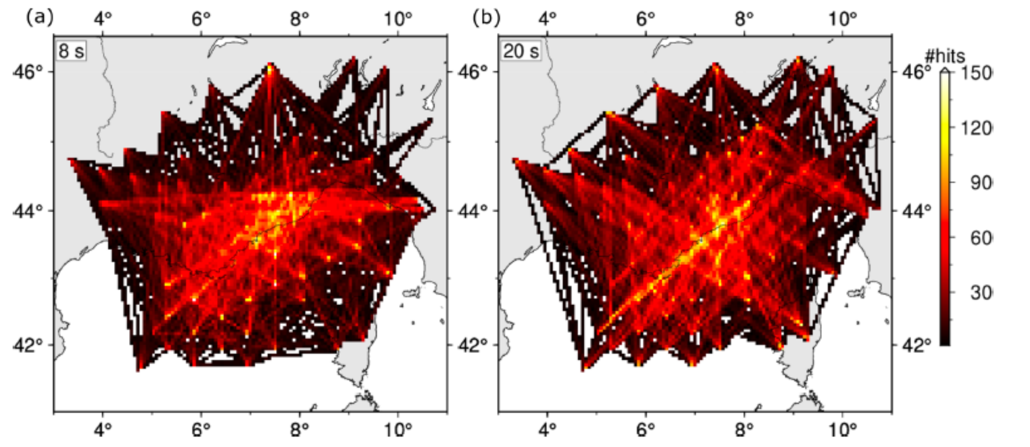

Fig. 6: *Hit count maps showing the ray coverage for ambient noise CCF pairs at 8 s (a) and teleseismic CCF pairs at 20 s (b).*

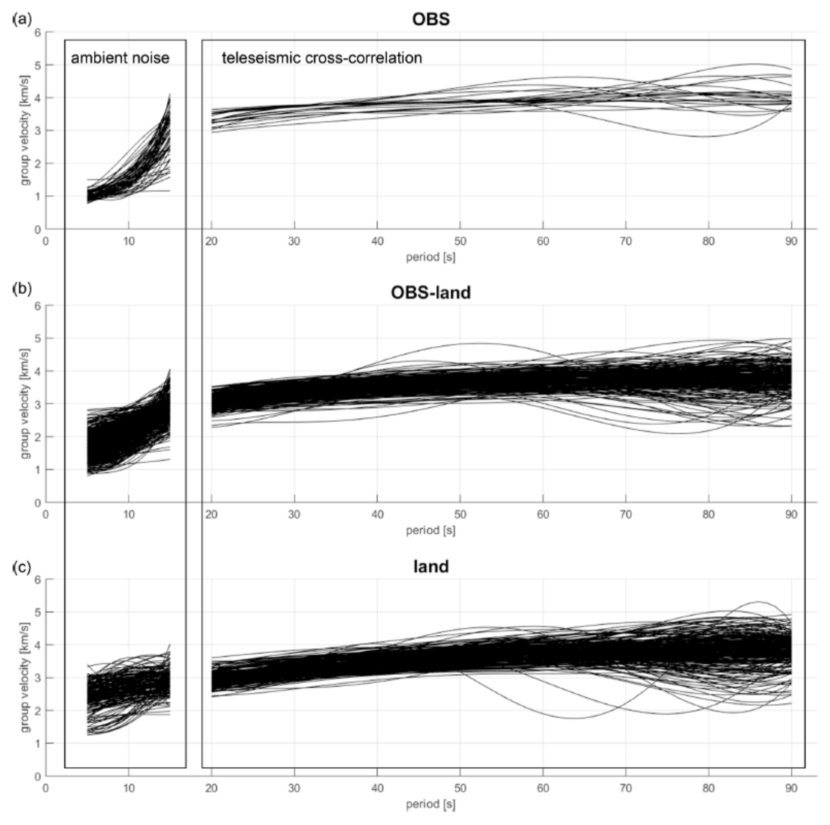

Fig. 7: *Picked dispersion curves from ambient noise cross-correlation and correlation of teleseismic events. The dispersion curves are sorted for different types of station pairs: (a) OBS–OBS pairs, (b) OBS–land pairs and vice versa, (c) land–land pairs.*

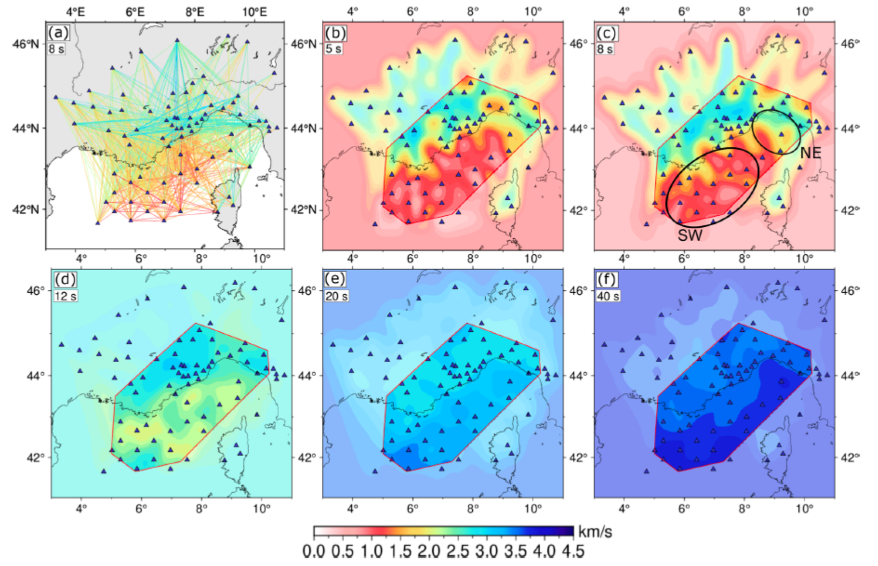

Fig. 8: *Group velocity maps for different periods. Panel (a) shows the tomography input for 8 s periods as a ray path plot. Panels (b), (c), and (d) are based on ambient noise cross-correlation and (e) and (f) are based on the cross-correlation of teleseismic events. A red polygon marks the resolved area. Areas of low resolution are shown in transparent colours; areas without ray coverage show the initial velocity. Annotations in (c) mark the south-western and central (SW) and the north-eastern (NE) Ligurian Basin.*

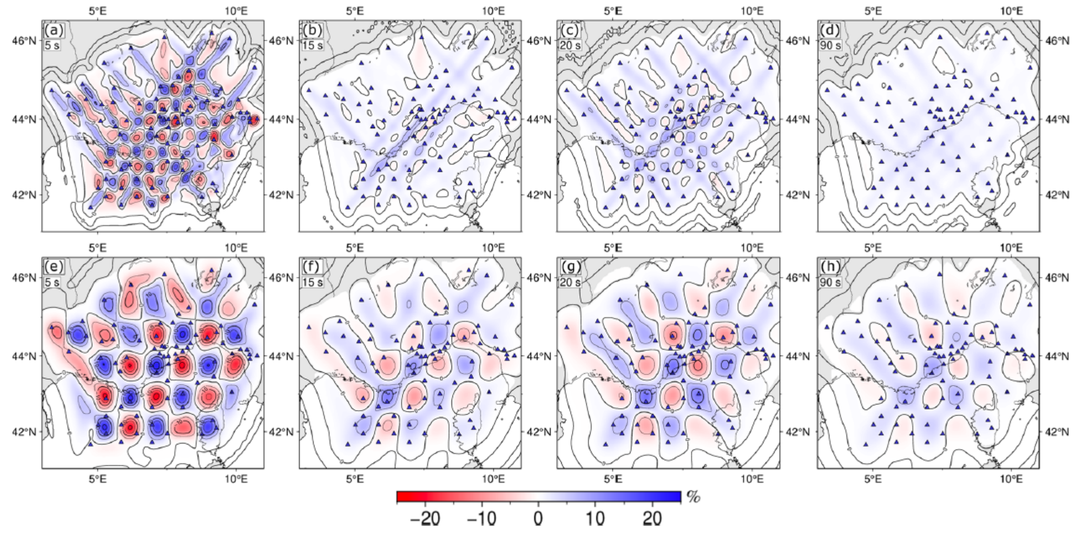

Fig. 8: *Checkerboard tests for periods of 5, 15 (both ambient noise cross-correlation), 20, and 90 s (both teleseismic cross-correlation). The perturbation of the input checkerboard tiles is set to 25 %. Panels (a)–(d) show checkerboard tests with a grid size of 0.4°x0.4°; panels (e)–(h) show a grid size of 0.8°x0.8°. The standard deviation of Gaussian noise (of travel times) is set to 0.375 s for (a) and (e), 0.665 s for (b) and (f), 0.708 s for (c) and (g), and 1 s for (d) and (h). Blue triangles represent stations.*

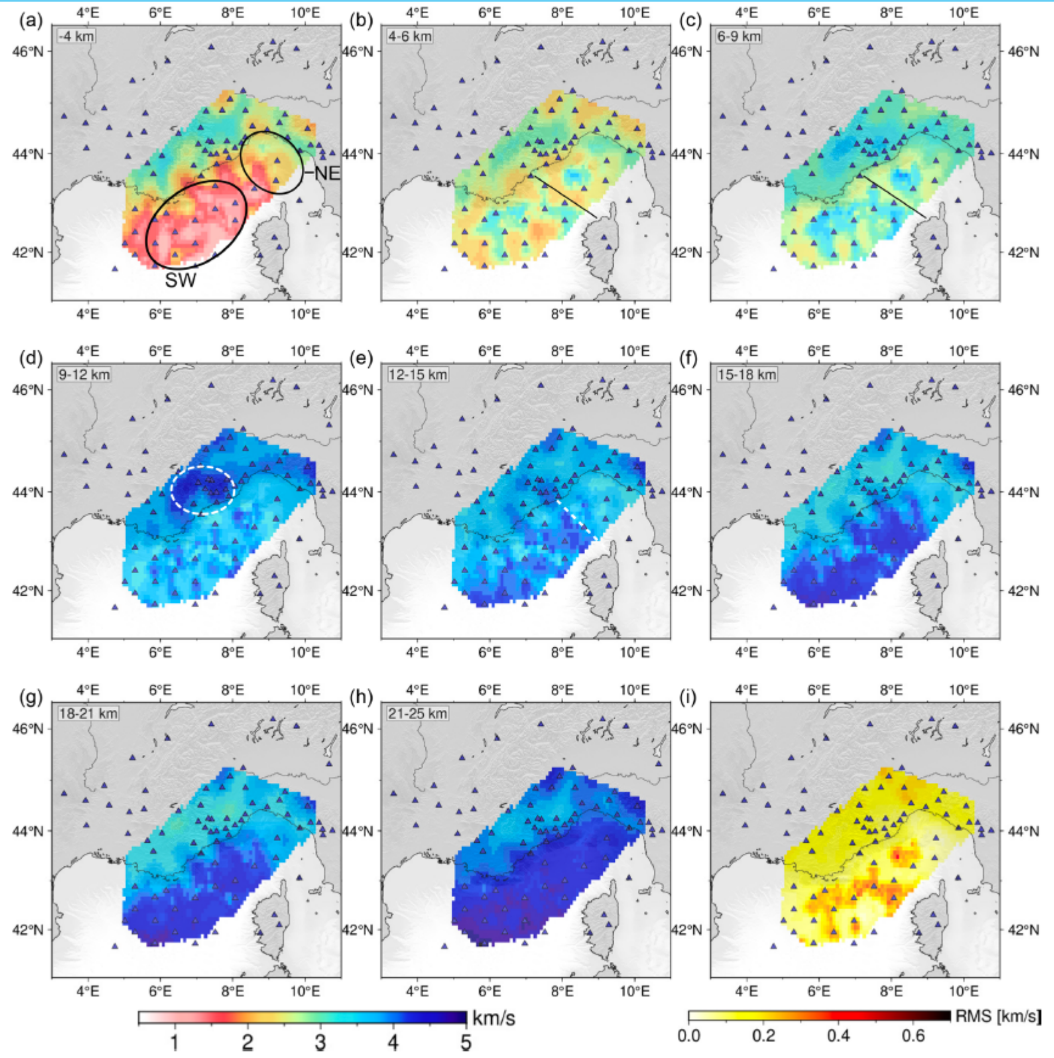

Fig. 9: *2D shear velocity maps derived from the 1D inversion. Layer depth is stated in the upper left corner. Depths (in km) are relative to the sea surface. The annotations in (a) mark the south-western and central (SW) and the north-eastern (NE) Ligurian Basin. The solid black line in (b) and (c) show the location of profile LISA01 (Contrucci et al., 2001). The dashed circle in (d) marks a high-velocity area north of Nice, and the dashed white line in (e) represents the proposed prolongation of the Alpine front (Rollet et al., 2002). Panel (i) shows the root mean square (RMS) value for the 1D shear-wave-inversion in map view (i.e. one RMS value per grid point). Blue triangles mark stations.*

References

- Bensen et al., 2007, DOI: 10.1111/j.1365-246X.2007.03374.x
- Bethoux et al., 2008, DOI: 10.1029/2007TC002232
- Craword et al., 1998, DOI: 10.1029/97JB03532
- Crawford and Webb, 2000, DOI: 10.1785/0119990121
- Dannowski et al., DOI: 10.5194/se-2019-187
- Dziewonski et al., A technique for the analysis of transient seismic signals, BSSA, 1969
- Herrman, 2013, DOI: 10.1785/0220110096
- Lustrino et al. (2011), DOI: 10.1016/j.earscirev.2010.08.002
- Rawlinson and Sambridge, 2005, DOI: 10.1071/EG05341
- Rollet et al., 2002, DOI: 10.1029/2001TC900027
- Schettino and Turco, 2006, DOI: 10.1111/j.1365-246X.2006.02997.x
- Wolf et al., 2021, DOI: , 2006, DOI: 10.5194/se-12-2597-2021

Acknowledgements
This project is funded by Deutsche Forschungsgemeinschaft (DFG), grant number LA 2970/3-1. We thank captain and crew of RV Pourquois Pas? and RV Maria S. Merian for their support during installation and recovery of the OBS array. We used 12 instruments from the German instrument pool DEPAS. We thank everybody in the AlpArray community for providing data (http://data.datacite.org/10.12686/alparray/z3_2015). We also use data from RESIF (http://doi.org/10.15778/RESIF.FR), Swiss Seismological Service (SED) (https://doi.org/10.12686/sed/networks/ch) and the INGV Seismological Data Centre (http://doi.org/10.13127/SD/X0FXnH7QfY). Further, we thank the AlpArray Seismic Network Team (http://www.alparray.ethz.ch/en/home). We would also like to thank the working group of Thomas Meier at Kiel University for providing software.

SPITZENFORSCHUNG FÜR GROSSE HERAUSFORDERUNGEN